View Online / Journal Homepage
Dynamic Article Links

Journal of Materials Chemistry

Cite this: DOI: 10.1039/c2jm15762d

www.rsc.org/materials

PAPER

Sulfonic groups induce formation of filopodia in mesenchymal stem cells†

Diana Soares da Costa,[ab] Ricardo A. Pires,[ab] Ana M. Frias,[ab] Rui L. Reis[ab] and Iva Pashkuleva*[ab]

Received 9th November 2011, Accepted 31st January 2012
DOI: 10.1039/c2jm15762d

Glycosaminoglycans (GAGs) are an integral part of the extracellular matrix and glycocalix, *i.e.* the closest cellular environment. They are abundant in –OH groups and their bioactivity is also associated with the presence of negatively charged $–SO_3H$ functionalities. Therefore, we have investigated and discussed the influence of these functional units on mesenchymal stem cells (MSCs) behaviour using single component and mixed self-assembled monolayers of alkanethiols with $–SO_3H$ and –OH end groups. In the absence of serum, MSCs attachment, spreading, cytoskeleton organisation and motility were significantly influenced by the surface chemistry. We found that the sulfonic groups induce star-like cell shape with very intense actin staining and a high density net of filopodia that enlarge from the base of lamellipodia structures. Moreover, this response is concentration dependent and is apparent only for very short culture time in the presence of serum.

Introduction

Mesenchymal stem cells (MSCs) are multipotent progenitor cells that have potential to differentiate into several cell lineages (*e.g.* adipocytes, osteocytes, chondrocytes, neurons, muscle cells, *etc.*) and capacity of self-renewal.[1–3] These properties of MSCs together with the possibility to isolate them in large quantities from bone marrow and recently from adipose tissue of adult patients highlight their potential as a cell source in different tissue regeneration and repair strategies.[3–6] The extracellular microenvironment of MSCs plays a significant role in the control of their fate. In addition to vastly investigated exogenous soluble factors (*e.g.* growth factors and cytokines), cell function can be also modulated by extracellular matrix (ECM) molecules.[7,8] Glycosaminoglycans (GAGs) are an integral part of the ECM. GAGs are anionic polysaccharides made of repeating disaccharide units. Their negative charge is generally associated with the presence of sulfonic groups. It is believed that those charged units have a crucial role in the formation of proteoglycans and therefore in key biochemical processes/signalling related to cell functionality and survival.[9–13] However, no complete molecular-level understanding exists to date about the mechanisms of the cell–cell and cell–ECM interactions involving GAGs. The complex physiological microenvironment in which those interactions occur is one of the main reasons that limited such studies. Hence, surfaces equipped with molecular cues mimicking certain aspects of structure or function of natural GAGs have been used for mechanistic studies of the pathways by which cells sense, integrate and respond to changes in their environments.[14–17] Different materials have been exploited for studies in cell biology. However, self-assembled monolayers (SAMs) of alkanethiolates on gold remain the most used model platform due to a number of advantages such as preparation simplicity, well defined surface chemistry and reproducibility, wide flexibility in attaching and patterning ligands and compatibility with different characterisation techniques.[18,19] Several studies investigating the MSCs behaviour on SAM surfaces with different functionalities have been recently reported.[6,20–23] Alkanethiolates embellished with bioactive peptide sequences[21–23] as end groups or with different functional groups (–OH,[6,20] $–NH_2$,[20] $–CH_3$,[6,20] and –COOH[20,21]) resulting in the formation of surfaces with different charge and wettability have been reported to influence MSCs proliferation and differentiation. Given the fact that the closest cellular environment (glycocalix and ECM) is abundant in $–SO_3H$ groups, the limited information that exists on the influence of these groups on MSC properties is surprising. Therefore, our motivation for this work was to elucidate and further investigate the effect of the chemical nature of the surface on stem cell behaviour with particular focus on $–SO_3H$ groups. We employed single component and mixed SAMs of alkanethiols $(HS(CH_2)_{11}X)$ with $–SO_3H$ and –OH end groups—the main functional groups present in the natural GAGs. Human MSCs from adipose tissue and bone marrow were cultured in direct contact with the obtained surfaces and their behaviour was compared at different levels. Here we discuss: (i) the effect of surface functional groups on cell adhesion, spreading and cytoskeleton organisation; (ii) behavioural differences for MSCs

[a]*3B's Research Group—Biomaterials, Biodegradables and Biomimetics, University of Minho, Headquarters of the European Institute of Excellence on Tissue Engineering and Regenerative Medicine, AvePark, 4806-909 Taipas, Guimarães, Portugal. E-mail: pashkuleva@dep.uminho.pt; Fax: +351 253 510909; Tel: +351 253 510907*
[b]*ICVS/3B's—PT Government Associate Laboratory, Braga/Guimarães, Portugal*

† Electronic supplementary information (ESI) available. See DOI: 10.1039/c2jm15762d

obtained from different sources and (iii) influence of serum proteins on the properties of MSCs in contact with SAM surfaces.

Materials and methods

11-Mercapto-1-undecanol (97%), 1,11-dibromoundecane (98%), sodium sulfite (98%) and thiourea (99%) were purchased from Sigma-Aldrich and used without further purification. 11-Mercaptoundecanesulfonic acid was synthesised adapting a previously reported procedure[24] (ESI†).

Preparation and characterisation of SAMs

The substrates used in this study were glass slides uniformly coated with gold (~20 nm) by the e-beam technique. Titanium (3–5 nm film) was used as a primer improving the adhesion between the gold and the glass.[18] The SAMs were formed by immersion of cleaned substrates (piranha solution, 30 min) into 20 μM ethanol solution of $HS(CH_2)_{11}OH$ (sample designated as SO_3H 0) or $HS(CH_2)_{11}SO_3H$ (sample SO_3H 100) for at least 48 h to ensure well formed monolayers (Fig. S2†). Mixed SAMs were formed by co-adsorption from binary solutions prepared by mixing pure solutions at $–SO_3H$: –OH ratios of 1 : 3 and 3 : 1 in order to obtain 25% and 75% of $–SO_3H$ groups on the surface. These samples are further referred to as SO_3H 25 and SO_3H 75, respectively. The coated substrates were washed several times with ethanol and dried under N_2 prior to characterisation.

The thiol coatings were analysed by contact angle goniometry, X-ray photoelectron spectroscopy (XPS) and time-of-flight secondary ion mass spectrometry (ToF-SIMS). Static contact angle measurements were performed using a contact angle meter OCA 15+ (DataPhysics Instruments, Germany) and the circle fit algorithm with a sessile drop of water (1 μL, HPLC grade). At least six contact angle replicates per sample were measured and averaged. The chemical composition of the samples was examined by XPS surface measurements. The C1s, S2p, O1s, Au4f, and survey spectra were recorded using a K-Alpha instrument (Thermo Scientific). The monochromatic X-ray source Al Kα (1486.6 eV) was used for all samples and experiments. Photoelectrons were collected from a take-off angle of 90° relative to the sample surface. The measurements were performed in a constant analyser energy mode (CAE) with a 100 eV pass energy for survey spectra and 20 eV pass energy for high resolution spectra. The sample charging was corrected by assigning a binding energy of 285.0 eV to the saturated hydrocarbons C1s peak. The atomic concentrations were determined from the XPS peak areas using the Shirley background subtraction technique and the Scofield sensitivity factors.

The mass spectra and mapping of the samples were recorded on a ToF-SIMS IV instrument (ION-TOF GmbH, Germany). The samples were bombarded with a pulsed bismuth ion beam (25 keV) at 45° incidence over an area with size of 250 μm^2. The generated secondary ions were extracted with a voltage of 10 kV and their mass was determined by measuring their time of flight from the sample to the detector. Negative secondary ion mass spectra were obtained using an acquisition time of 20 s and a mass range from $m/z = 0$ to $m/z = 1000$. The experimental conditions (ion type, beam voltage and primary ion dose) were maintained constant for comparative studies. Each map was obtained from an area of analysis 250 μm^2 and 35 scans.

Cell culture

The protocols for isolation and expansion of human bone marrow derived mesenchymal stem cells (BM-MSCs) and adipose stem cells (ASCs) are presented in the ESI†. Cells from the third and fourth passage were used in this study.

We have carried out two sets of experiments. In the first one we aimed to evaluate the effect of surface chemistry on cell adhesion, spreading, cytoskeleton organisation and motility. Thus, SAMs ($n = 3$ for each condition) were seeded either with BM-MSCs or ASCs at a concentration of 3000 cells cm^{-2} in serum free medium and incubated for 1, 7, and 24 h at 37 °C under a humidified atmosphere of 5% CO_2. The second set of experiments was conceived to assess the influence of proteins on the cell–surface interactions and therefore, it was carried out in a medium containing 10% FBS using the same cells concentration and the same sampling times. TCPS coverslips and gold-coated glass slides were processed as the other samples and used as controls. The number of cells per area was evaluated for all the samples after 1 h of incubation.

Cytoskeletal organisation and focal adhesions formation

After the above-mentioned incubation times expired, the samples were washed twice with PBS, fixed in 10% neutral buffered formalin for 30 min at 4 °C, permeabilised with 0.2% Triton X-100 in PBS for 5 min, and blocked with 3% BSA in PBS for 30 min at room temperature. To evaluate focal adhesion formation, a primary antibody against vinculin (clone h-VIN1, 1 : 400 in 1% w/v BSA/PBS, Sigma) was employed, followed by rabbit anti-mouse Alexafluor-488 (1 : 500 in 1% w/v BSA/PBS, Invitrogen). A phalloidin–TRITC conjugate was used (1 : 200 in PBS for 30 min, Sigma) to assess cytoskeleton organisation. Nuclei were counterstained with 1 μg mL^{-1} 4,6-diamidina-2-phenylin (DAPI; Sigma) for 30 min. Samples were washed with PBS, mounted with Vectashield® (Vector) on glass slides and observed under an Imager Z1 fluorescence microscope (Zeiss) and photographed using an Axio Cam MRm (Zeiss).

Cell migration

BM-MSCs (3000 cells cm^{-2}) were seeded (serum free medium) on SO_3H 100 and SO_3H 0 surfaces and incubated at 37 °C under an inverted microscope (Zeiss Axiovert200M) equipped with a temperature and CO_2 control device. Time-lapse images (10X) were captured every 10 min using an open source microscopy software Micro-Manager 1.47. Cells were continuously observed for 24 h. Image stacks were stitched and analysis of the migration paths was performed with image processing package Fiji (http://fiji.sc/wiki/index.php/Fiji). At least 10 non-dividing cells were tracked for each surface. Gold was used as a control. The obtained data were analysed as described in the Statistical analysis section.

Morphological analysis by scanning electron microscopy

Scanning electron microscopy (SEM) was employed to evaluate the morphological appearance of cells. The samples used for

immunostaining were washed twice in PBS, dehydrated in a graded series of ethanol, and finally, dried using hexamethyldisilazane. The samples were examined at an accelerating voltage of 15 kV in a Leica Cambridge S-360 scanning electron microscope. The size of the formed filopodia was measured using the micrographs of the cells cultured for 24 h.

Statistical analysis

All the quantitative results were obtained after analysis of at least six measurements per sample. Initially, a Shapiro–Wilk test was used to ascertain the normality of the data. When the data followed a normal distribution, the results were presented as mean ± standard deviation (SD). Student's *t*-tests for independent samples were performed to test differences among the samples. Box plot presentation of the data was used when they did not follow a normal distribution. The Kruskal–Wallis test followed by the Mann–Whitney test was applied in this case in order to determine the statistical significance of the observed differences. Throughout the following discussion, the differences were considered significant if $p < 0.05$.

Results and discussion

Formation and characterisation of SAMs

A combination of data from contact angle measurements, XPS and ToF-SIMS, was used for chemical characterisation of the formed SAMs. The contact angle values for the modified surfaces (Fig. 1A) were significantly different from the bare gold samples (83.5 ± 4.0°) demonstrating hydrophilic behaviour after the SAM deposition. The surfaces richer in –OH groups were more hydrophilic ($\theta_{SO_3H\_0} \approx 24°$ and $\theta_{SO_3H\_25} \approx 18°$) than the ones abundant in $-SO_3H$ groups ($\theta_{SO_3H\_75} \approx 31°$ and $\theta_{SO_3H\_100} \approx 33°$). These results are in agreement with previously reported data[24–26] for surfaces homogeneously modified with –OH or $-SO_3H$ groups, indicating that SAM formation was successful.

The obtained data were further confirmed by the results from the XPS analysis (Fig. 1B and C and Table S1†). The binding energies and the possible oxidation states of sulfur (S) were obtained from the high resolution XPS spectra of O1s and S2p. The S2p high resolution spectrum (Fig. 1C) shows two dominant peaks at 162.2 eV and 163.4 eV that are assigned to bound S atoms (S2p3/2 and S2p1/2) on the Au surface. An additional peak (168.1–169.5 eV) was detected for the samples obtained by the chemisorption from solutions containing $HS(CH_2)_{11}SO_3H$. This peak corresponds to oxidised S and its intensity increases with the augmentation of $HS(CH_2)_{11}SO_3H$ in the solution (Fig. 1B). In fact, the obtained values from the XPS are very close to the theoretically calculated ones which confirm the successful formation of SAMs from mixed and single component solutions.

We have also carried out ToF-SIMS analysis because this technique is more sensitive in comparison with XPS both in terms of detection and depth limits. The results confirmed that there is a clear increase in the oxidised S content with the increase of the concentration of $HS(CH_2)_{11}SO_3H$ in the immersing solution (Fig. 2).

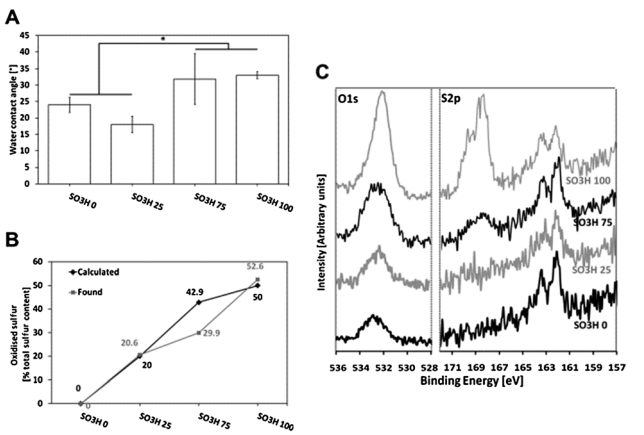

Fig. 1 Water contact angle values (A) and oxidised sulfur content (B) calculated from S2p3/2 high resolution XPS spectra (C) of the coated surfaces. The significant difference (Student's *t*-test, $p < 0.05$) is marked with *.

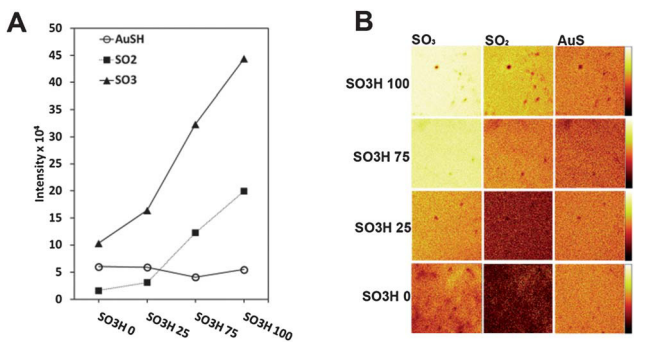

Fig. 2 ToF-SIMS data showing an increasing concentration of SO_2^+ ($m/z = 63.96$) and SO_3^+ ions ($m/z = 79.96$) for the samples SO_3H 0 to SO_3H 100 (A) and homogeneous distribution of these ions (B) on the studied surfaces (light colour corresponds to higher concentration).

Effect of surface chemistry on cell adhesion, spreading and cytoskeleton organisation

The influence of the obtained surface chemistries on BM-MSCs and ASCs behaviour was further evaluated. As it was expected, the cell adhesion, spreading and cytoskeleton organisation were strongly influenced by the surface chemistry in the absence of proteins (Fig. 3 and 4). When cultured in contact with hydroxyl terminated SAMs (SO_3H 0), the cells demonstrated a typical MSC shape with actin visible at the edge of the cellular borders and vinculin diffuse in the cytoplasm (Fig. 3 and 4A–C). After 7 h of culture, an organised cytoskeleton with assembled actin stress fibres can be already seen (Fig. S5 and S6†) although this effect was less pronounced for BM-MSCs. At the end of the culture period (24 h), vinculin was observed in both types of cells, but efficient FAs formation at the end of actin bundles[27] was only seen for ASCs when –OH functional groups were present on the surface (Fig. 4, green dots). Different cell morphology and proteins (actin and vinculin) expression pattern were observed for the cells cultured on the SO_3H 100 sample. After 1 h of culture, cells with star-like shape and very intense actin staining (Fig. S5 and S6†) demonstrating the presence of microspikes can be seen in Fig. 3J and 4J. Additionally, the vinculin staining was less intense especially in the case of BM-MSCs (Fig. 3A *vs.* 3J). Moreover, the typical organisation of actin filaments into barbed

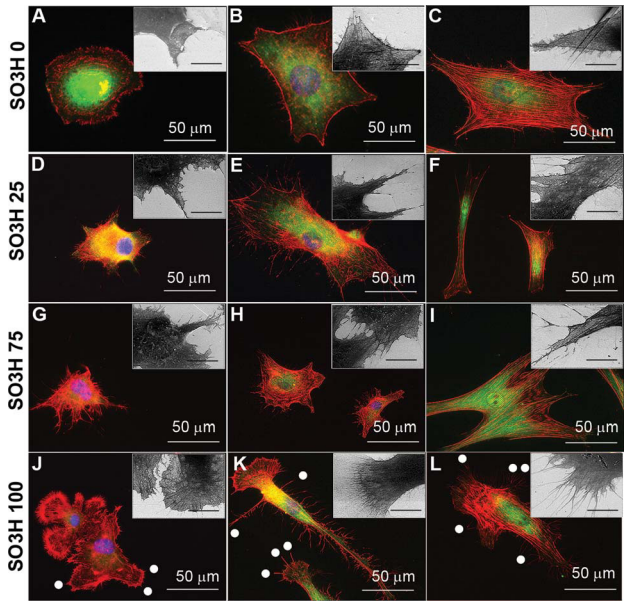

Fig. 3 Fluorescence microscopy images of BM-MSCs cultured in contact with SAMs with different –SO_3H content: immunostaining of vinculin (green), actin (red) and nuclei (blue). The insets correspond to SEM micrographs of the same samples (bars = 10 μm). The white dots indicate some filopodia edges.

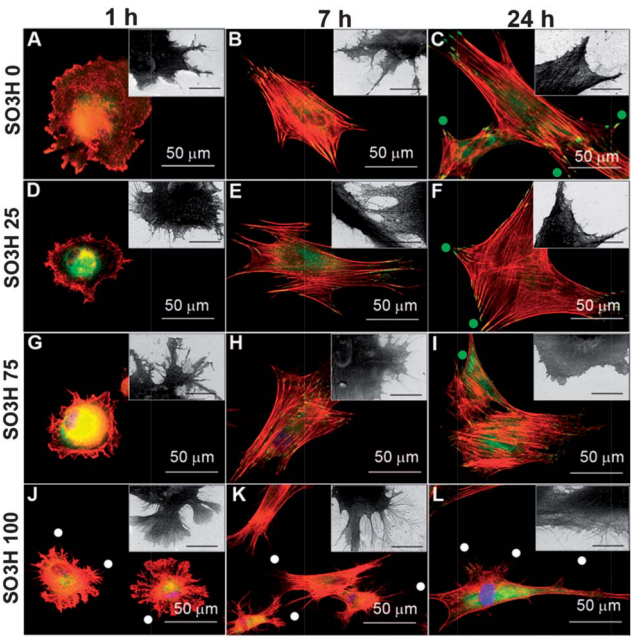

Fig. 4 Fluorescence microscopy images of ASCs cultured on surfaces with different –SO_3H content: immunostaining of vinculin (green), actin (red) and nuclei (blue). The insets correspond to SEM micrographs of the same samples (bars = 10 μm). The dots indicate some filopodia (white) and FA (green) edges.

ends was observed for this type of cells after 7 and 24 h of culture (Fig. 3K and L). The SEM analysis demonstrated that both BM-MSCs and ASCs exhibit a high density net of filopodia that grow with the prolongation of the culture time (Fig. 3 and 4J–L, insets).

Lamellipodia structures are also visible for both types of cells and for this surface chemistry (Fig. 3 and 4J–L, insets). Those structures were not observed for the cells cultured on SO_3H 0 and SO_3H 25. In the case of SO_3H 75 surfaces, some filopodia formation can be also seen but the effect was not as pronounced as for the SO_3H 100.

The morphology of the cells cultured on the control surfaces (gold and TCPS) is similar to the one observed for the SO_3H 0 surface (Fig. S3 and S4†) with faint vinculin staining and assembled actin stress fibres after 7 h of culture.

In the absence of serum (no adsorbed protein layer), cells do interact directly with the underlying surface. They do explore this new space by protrusion of actin rich organelles at their edge, followed by their adhesion to extracellular matrices and by cell body translocation. In all the cases, we have observed formation of actin filaments indicating an effective outside-in signalling between the material surface and the cells cultured on them.[28] However, the position and extension persistence of these filaments are different for BM-MSCs and ASCs cultured on surfaces with different chemistries. Our results suggest that different surface chemistries trigger different mechanisms[29,30] of actin stress fibres formation. In the case of SO_3H 100 surfaces, we presume that new actin fibres are generated mainly by elongation of existing filaments. When cells are in contact with –OH groups the nucleation of new filaments is the initial process followed by elongation of these filaments. Because elongation is kinetically favoured over the nucleation,[31] longer actin stress fibres are generated by the former mechanism. In fact, we have found a significant difference between the filopodia (tight bundles of long actin filaments oriented toward the protrusion) size of the cells cultured on SO_3H 0 and SO_3H 100 for 24 h (Fig. 5) with BM-MSC exhibiting the longest cytoplasmic projections when cultured in contact with –SO_3H groups alone.

Filopodia have been described as chemotropic antennae that are sensitive to environmental signals.[32,33] Previous studies[34,35] have reported that integrins accumulate in filopodia in an unligated but conformationally active state creating "sticky fingers" along the leading edge that promote cell adhesion and migration.[32,34] Thus, we have compared the migration ability of

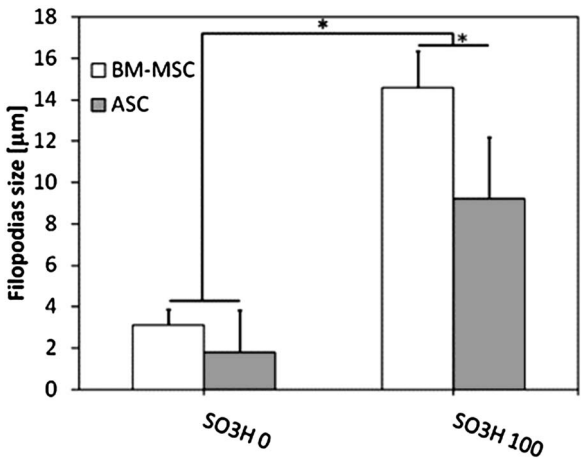

Fig. 5 Filopodia size determined from the SEM micrographs of BM-MSCs and ASCs cultured for 24 h on the respective surfaces. The significant differences (Student's *t*-test, $p < 0.05$) are marked with *.

BM-MSCs cultured on –OH and –SO_3H functionalised surfaces (Fig. 6 and ESI Movies†). The results demonstrated that BM-MSCs cultured on the SO_3H 100 surface do not only have longest filopodia but do also migrate significantly longer distances than on the SO_3H 0 surface.

Effect of adsorbed serum proteins on cell–surface interaction

In the presence of proteins, the very first event that occurs upon the contact of synthetic surfaces with biological fluids is a fast (seconds) and usually non-specific adsorption of proteins.[25,36] Other responses such as cell attachment and cytoskeleton organisation are secondary and governed by the nature of the adsorbed protein layer.

We have investigated and compared cell adhesion and spreading in the presence and absence of serum proteins using the above described surface chemistries. The results demonstrated that when BM-MSCs and ASCs are cultured on SAMs in serum free medium they do adhere and spread on all surfaces, independently of the terminal groups (Fig. 7A, 3 and 4). After 1 h of culture, more ASCs were counted than BM-MSCs and this difference was significant for all studied surface chemistries. The number of adherent cells drastically decreases in the presence of serum proteins and this effect was most pronounced for the –OH rich surfaces, *i.e.* SO_3H 0 and SO_3H 25 (Fig. 7B). Previous studies[25,37] have presented similar results for other types of cells. Whitesides and coworkers have demonstrated[38] that generally hydrophilic and overall electrically neutral functional groups make the surfaces resistant to the adsorption of proteins. Indeed, several groups[6,25,39,40] have shown that under competitive conditions (complex protein solutions) adhesive proteins such as fibronectin and vitronectin tend to bind less to uncharged, hydrophilic –OH surfaces. As a result cells do adhere poorly on these surfaces in contrast to supports functionalised with charged functional groups such as –NH_2 and –COOH.[25,26,41] Our results are in agreement with those reports. In the presence of proteins and for short culture time (1 h), we have observed significant influence of the surface chemistry on the number of adherent cells: surfaces abundant in polar and charged –SO_3H groups induced better cellular adhesion than surfaces richer in –OH groups (Fig. 7B).

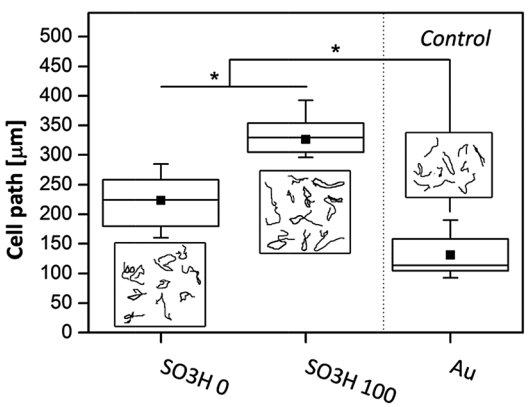

Fig. 6 Migration tracks (the insets) and the respective paths length calculated from the tracks for BM-MSCs over 24 h. The tracks of cells from 4 different fields of view have been compressed into each inset. The significant differences (Kruskal–Wallis test followed by the Mann–Whitney test, $p < 0.05$) are marked with *.

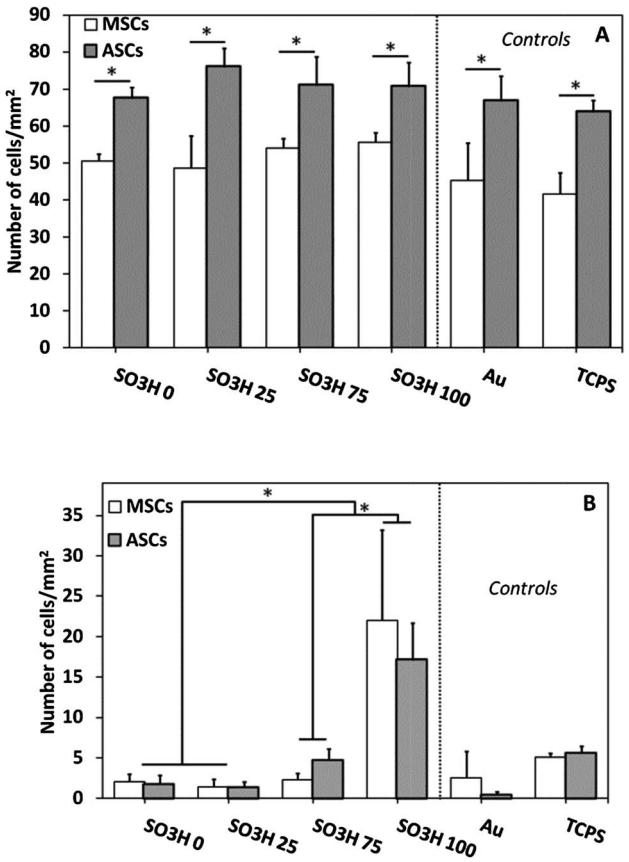

Fig. 7 Number of adherent cells after 1 h of culture in medium without (A) and with (B) serum proteins. The statistically significant difference (Student's *t*-test, $p < 0.05$) between BM-MSCs and ASCs (A) and between cells cultured on –SO_3H rich surfaces and –OH abundant ones (B) are marked with *.

The presence of proteins in the culture medium also induces different cytoskeleton organisation and protein expression patterns for BM-MSCs and ASCs (Fig. 8).

After 1 h of culture, actin can be seen throughout the cells cultured on different SAMs. At this time point, vinculin is visible only in the cells cultured on SO_3H 100; the staining revealed an establishment of FAs in the periphery of the cells (Fig. 8D and J). Few hours later, all cells exhibited very similar morphology comprising an organised cytoskeleton with well assembled actin fibres independently of the underlying surface chemistry. FAs were formed in the cells cultured on SO_3H 0 surfaces (Fig. 8B and H). The prolongation of the culture time to 24 h diminished any morphological differences induced by the surface chemistry and cells with similar shape, cytoskeleton organisation and well defined FAs can be seen at this time point. Similar results for BM-MSCs in contact with –OH surfaces have been previously reported.[42] Arima and Iwata have also observed this behaviour for endothelial cells.[41] They have explained it with an effective displacement of pre-adsorbed albumin (the most abundant protein in the serum) with cell adhesive proteins on hydrophilic SAMs.

The obtained results suggest that protein displacement also occurs on the surfaces studied by us and this process was more obvious for the most hydrophilic –OH surfaces. Upon exposure

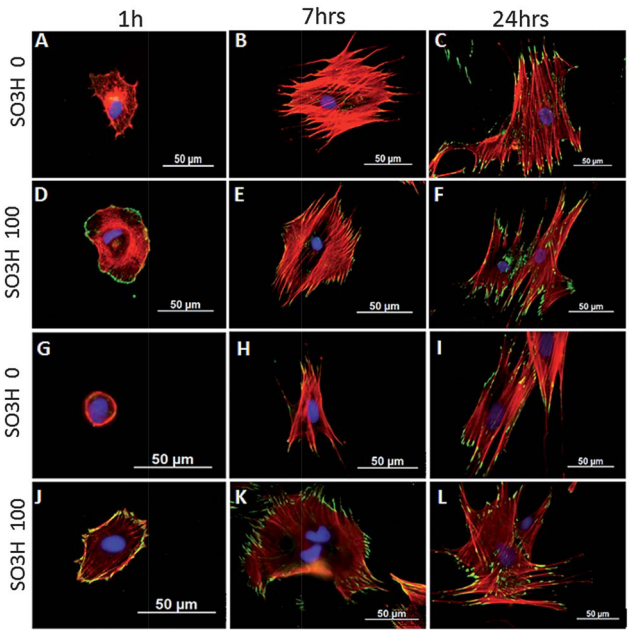

Fig. 8 Fluorescence microscopy images of BM-MSCs (A–F) and ASCs (G–L) cultured on single component SAMs: $HS(CH_2)_{11}OH$ and $HS(CH_2)_{11}SO_3H$. Immunostaining of vinculin (green), actin (red) and nuclei (blue).

to serum containing medium, albumin is expected to preferentially adsorb on the surfaces because of its high concentration (hundred to thousand times higher than those of fibronectin and vitronectin).

As a result, there are just few round cells with no FAs on SO_3H 0 surfaces at the initial studied period (1 h). Cell adhesive proteins effectively replaced the albumin and at the following time points these differences disappear. Thus, we can state that the surface chemistry influences the protein adsorption and cellular behaviour at very early stage but with the prolongation of the culture time the protein displacement masks the effect of the surface chemistry on the cell behaviour.

Sulfonic groups and GAGs mimicking

Our results suggest that the cells do sense the incorporated $–SO_3H$ groups on the surface and respond by changes in their morphology and motion. Moreover, this response is concentration dependent: the densest filopodia net and the longest cell paths were observed for the SO_3H 100 surface. Previous report from Granes *et al.*[43] demonstrated that overexpression of syndecan-2 (the most abundant heparan sulfate proteoglycan in fibroblasts) induces formation of long filopodia-like structures in COS-1 cells. The authors proved the critical role of the heparan sulfate extracellular domain in this process, *i.e.* in the control of actin polymerisation and filopodia formation. Here, we hypothesise that the sulfonic groups alone have the same influence on the BM-MSCs and ASCs morphology: they are inducing the formation of filopodia and/or are providing the appropriate molecular cues to activate specific signalling pathways.

Among the natural GAGs, heparin is the one with the highest content of $–SO_3H$ groups. The average heparin disaccharide contains 2.7 sulfonic groups resulting in a negative charge of approximately −75, *i.e.* one of the strongest acids in nature.[44] Its significance in the biomedical field was established based on its anticoagulant ability; the 3-O-sulfonic group on an internal GlcNpS6S residue is absolutely essential for its high affinity to antithrombin III.[45] Nowadays, a significant number of known heparin-binding proteins allows better characterisation of the recognition processes. Based on these studies, it is well established that the ionic interactions are crucial for the recognition; clusters of positively charged basic amino acids on proteins form ion pairs with spatially defined negatively charged sulfonic groups on the heparin chain.

The surfaces described in this work mimic the heparin structure by offering free $–SO_3H$ groups able to further interact with heparin-binding proteins. In fact, recent examples from the literature[46–48] demonstrate that addition of sulfonic groups to different biomaterials gives them high affinity to heparin-binding growth factors (*e.g.* FGF, VEGF) that in turn can induce sustained migration. In a serum free medium (no additive growth factors or other proteins), the metabolic cycle of BM-MSCs and ASCs involves the production of different proteins along the culture time.[49] Thus, a possible contribution of growth factors to the cell morphogenesis and migration can be speculated. However, there are two additional issues that must be considered. Although the surfaces studied by us contain the highly relevant $–SO_3H$ groups, the binding of growth factors also depends on GAG conformation, chain flexibility and molecular weight as well as on these hydrogen bonding and hydrophobic forces—factors which are not considered in our model surfaces. The second fact to be considered is that generally the growth factor–receptor interactions are important for long-term stimulation of signalling pathways[48] and, therefore, their contribution in such short culture periods as studied herein is likely to be less expressed.

Conclusions

Using well-defined SAMs of alkanethiols, we have investigated the effect of –OH and $–SO_3H$ groups on cell adhesion and morphology. We have demonstrated that sulfonic functional groups influence significantly cell morphology and mobility *via* modulation of the cytoskeleton organisation of both BM-MSCs and ASCs. In summary, the present study provides evidence that sulfonic groups induce formation of filopodia in stem cells independently of the source which these cells are isolated from. This effect is concentration dependent and observed only in a serum-free medium. In the presence of proteins, a significantly lower number of adherent cells was observed. Under these conditions, the effect of surface chemistry on the cellular behaviour (adhesion and morphology) was apparent only for very short culture time.

Acknowledgements

This work was carried out under the scope of the EU 7th Framework Programme (FP7/2007-2013) under grant agreement no. NMP4-SL-2009-229292 (Find&Bind). The authors gratefully acknowledge M. Carmen Márquez-Posadas and Santos Merino from Fundacion Tekniker for the provided gold coated glass slides. RAP and AMF acknowledge the Portuguese Foundation

for Science and Technology (FCT) for their post-doc grants (BPD/39333/2007 and BPD/45206/2008 respectively). The quadrupole ion trap mass spectrometer of ITN used in the characterisation of the obtained $HS(CH_2)_{11}SO_3H$ (Fig. S1†) was acquired with the support of the National Programme for Scientific Re-equipment of FCT and is a part of National network of mass spectroscopy (RNEM) also supported by FCT.

Notes and references

1 M. F. Pittenger, A. M. Mackay, S. C. Beck, R. K. Jaiswal, R. Douglas, J. D. Mosca, M. A. Moorman, D. W. Simonetti, S. Craig and D. R. Marshak, *Science*, 1999, **284**, 143–147.
2 X. B. Fu, Y. L. Si, Y. L. Zhao, H. J. Hao and W. D. Han, *Ageing Res. Rev.*, 2011, **10**, 93–103.
3 B. Parekkadan and J. M. Milwid, *Annu. Rev. Biomed. Eng.*, 2010, **12**, 87–117.
4 A. I. Caplan, *J. Cell. Physiol.*, 2007, **213**, 341–347.
5 A. Schaffler and C. Buchler, *Stem Cells*, 2007, **25**, 818–827.
6 C. C. Barrias, M. C. L. Martins, G. Almeida-Porada, M. A. Barbosa and P. L. Granja, *Biomaterials*, 2009, **30**, 307–316.
7 E. Alsberg, H. A. von Recum and M. J. Mahoney, *Expert Opin. Biol. Ther.*, 2006, **6**, 847–866.
8 F. Guilak, D. M. Cohen, B. T. Estes, J. M. Gimble, W. Liedtke and C. S. Chen, *Cell Stem Cell*, 2009, **5**, 17–26.
9 J. Pan, Y. Qian, X. D. Zhou, H. Lu, E. Ramacciotti and L. J. Zhang, *J. Biol. Chem.*, 2010, **285**, 22964–22973.
10 V. A. Lawson, B. Lumicisi, J. Welton, D. Machalek, K. Gouramanis, H. M. Klemm, J. D. Stewart, C. L. Masters, D. E. Hoke, S. J. Collins and A. F. Hill, *PLoS One*, 2010, **5**, e12351.
11 X. B. Ai, A. T. Do, O. Lozynska, M. Kusche-Gullberg, U. Lindahl and C. P. Emerson, *J. Cell Biol.*, 2003, **162**, 341–351.
12 M. Siczkowski, D. Clarke and M. Y. Gordon, *Blood*, 1992, **80**, 912–919.
13 T. Nagira, M. Nagahata-Ishiguro and T. Tsuchiya, *Biomaterials*, 2007, **28**, 844–850.
14 M. Mrksich, *Chem. Soc. Rev.*, 2000, **29**, 267–273.
15 M. Mrksich, *Acta Biomater.*, 2009, **5**, 832–841.
16 L. L. Kiessling and R. A. Splain, *Annu. Rev. Biochem.*, 2010, **79**, 619–653.
17 I. Pashkuleva and R. L. Reis, *J. Mater. Chem.*, 2010, **20**, 8803–8818.
18 J. C. Love, L. A. Estroff, J. K. Kriebel, R. G. Nuzzo and G. M. Whitesides, *Chem. Rev.*, 2005, **105**, 1103–1170.
19 A. Pulsipher and M. N. Yousaf, *ChemBioChem*, 2010, **11**, 745–753.
20 J. E. Phillips, T. A. Petrie, F. P. Creighton and A. J. Garcia, *Acta Biomater.*, 2010, **6**, 12–20.
21 W. Luo, E. W. L. Chan and M. N. Yousaf, *J. Am. Chem. Soc.*, 2010, **132**, 2614–2621.
22 J. T. Koepsel and W. L. Murphy, *Langmuir*, 2009, **25**, 12825–12834.
23 G. A. Hudalla and W. L. Murphy, *Langmuir*, 2010, **26**, 6449–6456.
24 J. C. Lin and W. H. Chuang, *J. Biomed. Mater. Res.*, 2000, **51**, 413–423.
25 Y. Arima and H. Iwata, *J. Mater. Chem.*, 2007, **17**, 4079–4087.
26 Y. J. Ren, H. Zhang, H. Huang, X. M. Wang, Z. Y. Zhou, F. Z. Cui and Y. H. An, *Biomaterials*, 2009, **30**, 1036–1044.
27 J. D. Humphries, P. Wang, C. Streuli, B. Geiger, M. J. Humphries and C. Ballestrem, *J. Cell Biol.*, 2007, **179**, 1043–1057.
28 K. B. McClary and D. W. Grainger, *Biomaterials*, 1999, **20**, 2435–2446.
29 J. Faix and K. Rottner, *Curr. Opin. Cell Biol.*, 2006, **18**, 18–25.
30 B. Geiger, J. P. Spatz and A. D. Bershadsky, *Nat. Rev. Mol. Cell Biol.*, 2009, **10**, 21–33.
31 T. J. Mitchison and L. P. Cramer, *Cell*, 1996, **84**, 371–379.
32 P. K. Mattila and P. Lappalainen, *Nat. Rev. Mol. Cell Biol.*, 2008, **9**, 446–454.
33 K. J. Jang, M. S. Kim, D. Feltrin, N. L. Jeon, K. Y. Suh and O. Pertz, *PLoS One*, 2010, **5**, e15966.
34 C. G. Galbraith, K. M. Yamada and J. A. Galbraith, *Science*, 2007, **315**, 992–995.
35 M. A. Partridge and E. E. Marcantonio, *Mol. Biol. Cell*, 2006, **17**, 4237–4248.
36 M. Mrksich and G. M. Whitesides, *Annu. Rev. Biophys. Biomol. Struct.*, 1996, **25**, 55–78.
37 M. Franco, P. F. Nealey, S. Campbell, A. I. Teixeira and C. J. Murphy, *J. Biomed. Mater. Res.*, 2000, **52**, 261–269.
38 E. Ostuni, B. A. Grzybowski, M. Mrksich, C. S. Roberts and G. M. Whitesides, *Langmuir*, 2003, **19**, 1861–1872.
39 A. S. Curtis and J. V. Forrester, *J. Cell Sci.*, 1984, **71**, 17–35.
40 N. Faucheux, R. Schweiss, K. Lutzow, C. Werner and T. Groth, *Biomaterials*, 2004, **25**, 2721–2730.
41 Y. Arima and H. Iwata, *Biomaterials*, 2007, **28**, 3074–3082.
42 J. M. Curran, R. Chen and J. A. Hunt, *Biomaterials*, 2005, **26**, 7057–7067.
43 F. Granes, R. Garcia, R. P. Casaroli-Marano, S. Castel, N. Rocamora, M. Reina, J. M. Urena and S. Vilaro, *Exp. Cell Res.*, 1999, **248**, 439–456.
44 I. Capila and R. J. Linhardt, *Angew. Chem., Int. Ed.*, 2002, **41**, 391–412.
45 U. Lindahl, G. Backstrom, L. Thunberg and I. G. Leder, *Proc. Natl. Acad. Sci. U. S. A.*, 1980, **77**, 6551–6555.
46 H. D. Maynard and J. A. Hubbell, *Acta Biomater.*, 2005, **1**, 451–459.
47 I. Freeman, A. Kedem and S. Cohen, *Biomaterials*, 2008, **29**, 3260–3268.
48 R. Mammadov, B. Mammadov, S. Toksoz, B. Aydin, R. Yagci, A. B. Tekinay and M. O. Guler, *Biomacromolecules*, 2011, **12**, 3508–3519.
49 D. Docheva, C. Popov, W. Mutschler and M. Schieker, *J. Cell. Mol. Med.*, 2007, **11**, 21–38.